

---

# ACT BETTER BY TIMING: A TIMING-AWARE REINFORCEMENT LEARNING FOR AUTONOMOUS DRIVING

---

Guanzhou Li<sup>1</sup>    Jianping Wu<sup>1,2,3</sup>    Yujing He<sup>1</sup>

<sup>1</sup>Tsinghua University    <sup>2</sup>Tsinghua University Research Institute at Shenzhen    <sup>3</sup>Sichuan Tianfu Yongxing Laboratory  
ligz19@mails.tsinghua.edu.cn    jianpingwu@tsinghua.edu.cn    hyj19@mails.tsinghua.edu.cn

## ABSTRACT

Coping with intensively interactive scenarios is one of the significant challenges in the development of autonomous driving. Reinforcement learning (RL) offers an ideal solution for such scenarios through its self-evolution mechanism via interaction with the environment. However, the lack of sufficient safety mechanisms in common RL leads to the fact that agent often find it difficult to interact well in highly dynamic environment and may collide in pursuit of short-term rewards. Much of the existing safe RL methods require environment modeling to generate reliable safety boundaries that constrain agent behavior. Nevertheless, acquiring such safety boundaries is not always feasible in dynamic environments. Inspired by the driver's behavior of acting when uncertainty is minimal, this study introduces the concept of action timing to replace explicit safety boundary modeling. We define "actor" as an agent to decide optimal action at each step. By imaging the actor take opportunity to act as a timing-dependent gradual process, the other agent called "timing taker" can evaluate the optimal action execution time, and relate the optimal timing to each action moment as a dynamic safety factor to constrain the actor's action. In the experiment involving a complex, unsignaled intersection interaction, this framework achieved superior safety performance compared to all benchmark models.

**Keywords** Reinforcement Learning, timing-aware RL, Safe RL, Model-based RL, Autonomous Driving

## 1 Introduction

As an emerging technology, autonomous driving is expected to enhance traffic safety by preventing accidents caused by human errors such as distracted driving. With substantial research and investment, autonomous driving systems perform well in most common scenarios, but their capability for sustained long-term driving still falls short of human performance [1], especially in interaction-intensive long-tail scenarios.

The rule-based and deterministic models widely used in the autonomous driving industry struggle to handle the nearly infinite variety of road environments, often resulting in overly conservative strategies that hinder vehicle progress in complex interactive situations. As an alternative technological route, learning-based methods can derive driving strategies by imitating human drivers or interacting with the environment. End-to-end autonomous driving, which integrates perception, planning, and decision-making, has demonstrated adaptability across various scenarios [2, 3]. However, in densely interactive situations, mimicking human driving behavior demands extensive interaction data, which is difficult to obtain and poses significant risks. Reinforcement learning (RL), a method of self-evolution through environmental interaction, excels in various domains including autonomous driving [4–6], able to learn interaction skills without requiring additional data. It has also been shown to enhance the performance and robustness of established strategies obtained through imitation learning or supervised learning [7]. Undoubtedly, as autonomous vehicles become more intelligent, RL will play an increasingly critical role in improving their interactive capabilities.

Reinforcement learning improves strategies through continuous trial and error in the environment, requiring considerable time and sophisticated reward design to succeed in complex, dynamic settings. The design of rewards in RL for autonomous driving faces the trade-off between efficiency and safety, and irrational reward design can lead to the dilemma between overly aggressive driving or action freezing, making vehicle fail to complete the tasks. To ensure safety and efficiency, safe RL introduces additional constraints, such as hierarchical mechanism allowing agent to

learn behavioral principles at the abstract macro level through a hierarchical approach [8, 9], limiting the potential risk probability of action [10–12], and introducing safety checkers [13]. Moreover, incorporating world models in RL can map environmental observations to low-dimensional latent spaces, enabling better predictions of future states and handling uncertainties more effectively [14–16]. Most of these methods require accurate estimation and modeling of the potential risks or future environmental dynamics to provide reliable safety constraints for autonomous vehicles. In practical driving tasks, drivers are not bound to quantify the future evolution of environment, but rather stay in safe state until the optimal timing with less uncertainty to execute the task. The choice of the optimal timing incorporates the driver’s implicit expectation about the future environmental dynamics instead of explicit complicated modeling.

This study proposes a timing-aware model-based reinforcement learning framework, consisting of two agents and a baseline policy. The two agents are called "actor" and the "timing taker" respectively. The actor generates the optimal action for the current state through reinforcement learning, while the baseline model always adopts the most conservative strategy. Such conservative strategies are prevalent in reinforcement learning tasks, for instance, the autonomous vehicle should employ car-following model without lane changing on straight road, or it should always wait at the stop line until there are no conflicting vehicles. These conservative strategies ensure high safety but may prevent the agent from completing the given tasks. The timing taker is responsible to connect the actions to maintain safety and actions to seize the opportunity to complete tasks through a timing-dependent gradual function. The projection of this gradual function at each moment determines the weighing ratio between the actor-generated action and baseline action, with the dynamic ratio referred to as "timing factor". The timing taker learns to estimate the optimal timing in a parallel environment through sparse opportunity-taking execution of the actor’s actions, and this process is called "timing imagination".

Some model-based safe reinforcement learning methods evaluate the current state by risk probability or costs to select either the baseline or learned action, which often merely mask unsafe action and the actor does not gain experience from the baseline strategy. The proposed framework realize a "soft" integration of baseline and learned actions through timing imagination, enable the actor to enhance its strategy through a better understanding of when should be conserved and when should act. Besides, the timing taker can be considered to operate depth-first search along the state tree, which can discover more valuable future states in a sparse reward environment. For continuous tasks like autonomous driving, where "survival" to the destination is the primary goal, this method can overcome the agent’s short-sightedness affected by short-term rewards, thereby effectively ensuring the safety of behaviors.

The main contributions of this study include:

- 1 A timing-aware model-based reinforcement learning framework is proposed, which enhance the safety of agent’s actions by introducing a "timing factor" determined by the optimal timing of action execution in the RL framework.
- 2 In this framework, an opportunity taker is designed to find the optimal execution timing for actor agent and learns the timing capability by "timing imagination".
- 3 The proposed model is compared with classic RL model and model-based DQN in a complex unsignaled intersection and exhibits outstanding performance and convergence speed.

The rest of this paper is organized as follows: Section 2 introduces the application of reinforcement learning in the field of autonomous driving, Section 3 details the specific methods of this study, Section 4 describes the experimental design and results, and Section 5 presents the conclusions and future prospects of this work.

## 2 Related Works

As the levels of autonomous driving advance, the number of scenarios that the vehicle must adapt to increases exponentially, making it challenging to enhance vehicle capabilities solely through human demonstration or manually devised rules. Reinforcement learning is poised to play an indispensable role in high-level autonomous driving, particularly in scenarios requiring dense interaction with surrounding traffic participants. For instance, [17] integrates spatio-temporal attention into the Deep Deterministic Policy Gradient (DDPG) algorithm, allowing the agent to focus more on traffic participants that significantly impact the ego vehicle’s motion, thus facilitating the lane-changing ability in dense traffic flow. [18] employs Graph Attention Networks (GAT) to model interactions between vehicles and uses Convolutional Neural Networks (CNNs) to extract bird’s eye view of the surroundings, and feeds the information into Deep Q Networks (DQN) to manage interactions across various traffic scenarios. Given that autonomous vehicle needs to balance safety, efficiency, and comfort during interactions, [19] designs a multi-objective reward to control the speed of vehicle using DDPG.

The dynamic nature of interactive environments complicates the interaction process in RL, necessitating enhanced exploration capabilities and accelerated convergence. RL can improve interaction proficiency by incorporating game

theoretic models or human priors. For example, DQN is used to model the behavior of agents at different levels in level-k games [20], and the Nash equilibrium solver is combined with DQN to address merging maneuvers on ramps [21]. However, modeling interactions between ego vehicle and surrounding vehicles through game theory faces difficulty in scaling up to more participants, and does not necessarily guarantee reaching equilibrium in sophisticated interactions. Human demonstrations can guide reinforcement learning to find appropriate actions faster. [22] constrains the deviation between RL policies and expert policies through KL divergence, exhibiting improved sample efficiency in sparse reward environments. [23–25] have found that hierarchical models combining RL and imitation learning are able to better utilize and enhance human driving demonstrations, and [26] avoids the reliance on human demonstrations by imitating the past optimal behaviors of agent itself as a robust baseline policy. To facilitate interactive ability in multi-class scenarios, tactical RL learns in the motion skill space instead of direct control maneuvers, then decodes the skills to specific actions through skill decoders [27, 28].

Despite the various methods that have been developed to enhance the interactive capability of RL, they generally lack inherent mechanisms to ensure the ego vehicle’s safety, while safety is the critical principle in autonomous driving, and the tolerance for task failure in autonomous driving is much lower than in most other RL applications. Consequently, safe RL has received a growing interest in the field of autonomous driving. Here we categorize safe RL in autonomous driving into: risk-constrained RL, hierarchical RL, adversariality enhanced RL, trustworthy RL, and expectation-based RL.

Risk-constrained RL employs cost functions to represent the agent’s future risk levels, ensuring safety by minimizing risk or keeping expected cumulative cost within a threshold. [29] establishes a Bayesian-based risk assessment model to evaluate state risk levels by state uncertainties and relative distances between the ego and surrounding vehicles, motivating the agent to learn policy that minimize expected risk. The Lagrangian method is more commonly used in risk constrained RL [30], coupling the process of seeking high-value states and avoiding high-risk states through Lagrange multipliers. However, Lagrangian-based safe RL is prone to a policy oscillation issue leading to performance decay. This issue can be addressed by dynamically adjust weight coefficients based on current and historical risk levels, aiming to avoid overly conservative policies while maintain safety [31, 32]. In addition to Lagrangian method, [33] proposed the concept of approximate safe action, encouraging to search for the closest action to original output of RL with the risk less than threshold.

Hierarchical safe RL introduces an additional safety-check layer or a safety-execution layer. The safety-check layer checks whether actions are safe and shields unsafe actions [34], while the safety-execution layer projects actions into safe sets [35, 36]. For the former, control barrier functions (CBF) is usually used to design safety shields for RL output to prevent the unsafe action [13], but the mean to distinguish safe actions from unsafe ones might not be always easy to describe in complex environments. For the latter, RL typically learns high-level driving strategies, while low-level strategies, including Model Predictive Control (MPC) [37, 38], Monte Carlo Tree Search (MCTS) [39, 40], and finite state machines [9], ensure the safety and kinematic feasibility of actions. In [8], a three-layer planning framework has been proposed, where the top layer uses Double DQN for macro strategy, the middle layer generates variable-length trajectory points, and a PID controller follows these trajectory points in the lower layer. Adversariality enhanced RL introduces adversariality or perturbations into the training process of RL to enhance the agent’s ability to combat extreme environmental disturbances [41, 42]. Trustworthy RL, often model-based, activates the learned policy when it guarantees an improvement on the baseline policy with a certain confidence level [6, 11, 43, 44], and it often requires intensively sampling to estimate confidence level at each step.

The final category, expectation-based RL, involves belief RL and curiosity-driven RL, the former estimates the probability that the environment will reach expectation state considering historical evolution paths [45], and the latter inspires the agent to explore states where prediction model performs poorly to improve adaptability and the likelihood of discovering high-value states [46, 47]. As a type of emerging technologies in expectation-based RL, world model has been demonstrated to improve the performance of RL including safety and interaction efficiency by encoding observations into a low-dimensional latent space [15, 48–50]. The latent space allows for better and more concise representations of environmental features and provides the agent with a clearer anticipation of the future evolution of the environment, leading to more accurate and reasonable actions. Considering that the prediction on the future dynamics of interactive environments remains challenging due to uncertainties, this study implicitly anticipates the environment through the concept of "timing" and achieves competitive results in terms of driving safety.

### 3 Methodology

This study proposes a timing-aware reinforcement learning framework, defined by six-variable tuple  $(S, A, D, P, R, \gamma)$ , where  $S$  represents the observation space,  $A, D$  denote the set of learned actions  $a$  at each step and the set of expected execution time  $T$  of the action  $a$ ,  $P, R, \gamma$  represent the transition probabilities between states, reward space, and the

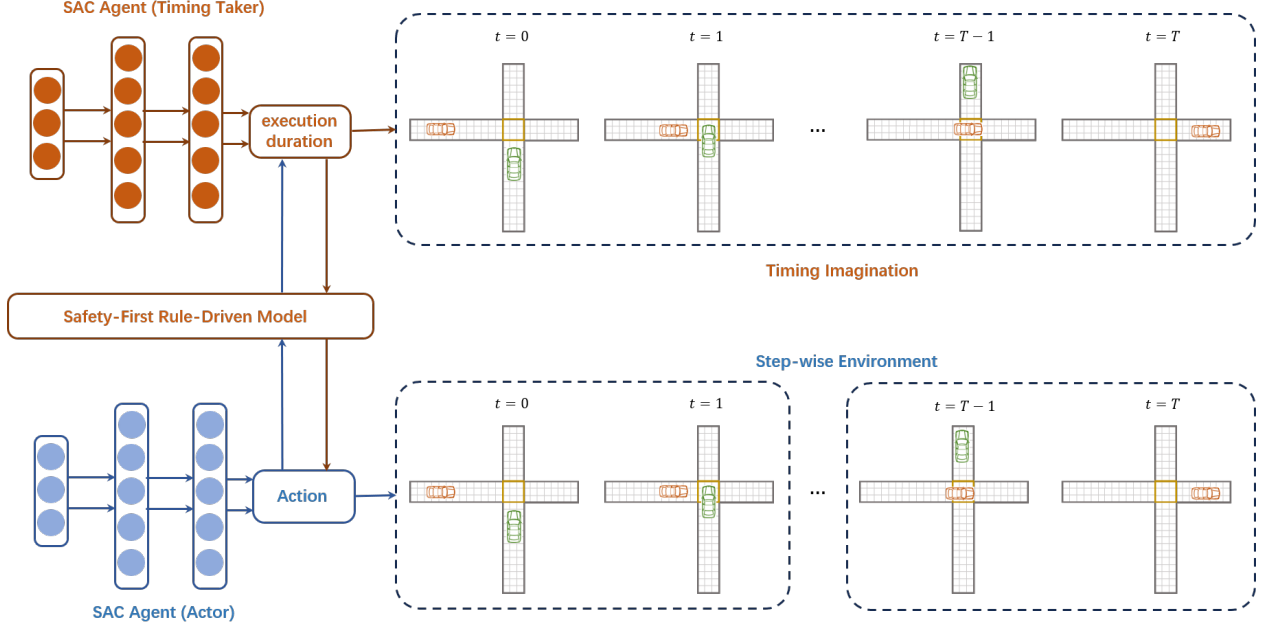


Figure 1: The Timing-aware Reinforcement Framework for Autonomous Driving

discount factor for future rewards, respectively. Two Soft Actor-Critic (SAC) agents are employed to generate action  $a$  and expected execution time  $T$ , and these two agents are called "actor" and "timing taker", whose policies are denoted as  $\pi_{\phi_a}, \pi_{\phi_T}$ . Beyond the two SAC agents, the framework implements a baseline model that always adopts more conservative strategy to keep in a safety state, whose action denoted as  $a_{base} \sim \pi_b$ . From the current moment to the expected execution time  $T$ , a progressively varying factor  $\beta$  denotes the gradual transition of the action employed by ego vehicle from the conservative action  $a_b$  to the actor-generated action  $a$ , and the factor  $\beta$  is called "timing factor", determined by the expected execution time  $T$  and the relative time step  $\Delta t$  within each expected execution duration from 1 to  $T$ , expressed as Eq. 1.

$$\beta(T, \Delta t) = \frac{1 - \cos[(1 - \frac{\Delta t}{T}) \cdot \pi]}{2}, \Delta t = 1, 2, \dots, T \quad (1)$$

The shorter expected execution time  $T$  is, the larger  $\beta$  will be at the beginning, indicating that the current or recent is more likely to be a favorable opportunity to perform the actor-generated action  $a$ , otherwise, and vice versa, indicating that a conservative strategy should be maintained. We define the process that the vehicle gradually performs the target action  $a$  according to the "timing factor"  $\beta(T, \Delta t)$  as Eq. 2.

$$\bar{a} = \beta(T, \Delta t) \cdot a + (1 - \beta(T, \Delta t)) \cdot a_{base} \quad (2)$$

where  $\bar{a}$  denotes the action actually executed by the vehicle at each time step, and the value of  $\beta$  will gradually converge to 1 as the  $\Delta t$  increases, representing that the executed action is gradually approaching the actor-generated action  $a$  from the conservative baseline action  $a_{base}$ . Since the length of action execution is different for "actor" agent and "timing taker" agent, actor is trained in the actual step-wise environment, while timing taker is trained in the environment where the expected execution time  $T$  is considered as a single action step. To distinguish these two parallel environments, the training environment of timing taker, where actions are not actually executed in reality, is called "timing imagination".

In "timing imagination", the timing taker will output a new expected execution period at the end of last execution period, noting the expected execution time output at moment  $t$  as  $T(t)$ . The actor will also output the optimal action  $a(t)$  at the same time, and it will remain unchanged during each expected execution period, so the action adopted by the vehicle at each time-step in "timing imagination" should be expressed as Eq. 3.

$$\bar{a}(t + \Delta t) = \beta(T(t), \Delta t) \cdot a(t) + (1 - \beta(T(t), \Delta t)) \cdot a_{base}(t + \Delta t) \quad (3)$$

In "timing imagination", only the gradient of the time taker is updated, and its Q-function can be expressed as Eq. 4, while the optimization objective function of its policy network is expressed as Eq. 5, and  $D_{replay}$  represents the memory replay buffer in SAC training, where a double Q network is used to estimate the value of state-action pairs, and the temperature coefficient  $\alpha$  is updated following the auto-tuning method in SAC.

$$Q_T(s(t), a(t), T(t)) \leftarrow \sum_{\Delta t=1}^{T(t)} \gamma^{\Delta t-1} r(s(t+\Delta t), \bar{a}(t+\Delta t)) + \gamma^{T(t)} \mathbb{E}_{s_{t+T} \sim P} [\hat{Q}_T(s(t+T), a(t+T), T(t+T))] \quad (4)$$

$$J(\phi_T) = \mathbb{E}_{s, a \sim D_{replay}, T \sim \pi_{\phi_T}} [Q^{\pi_{\phi_T}}(s, T) - \alpha \cdot \log \pi_{\phi_T}(T|s, a)] \quad (5)$$

Since the environment changes rapidly in the interaction scenarios, the actor needs to produce action at every time step in the actual environment to better react to the various behaviors of the surrounding traffic participants. In such environment, we always take  $\Delta t = 1$  in Eq 1, representing the opportunity expectation for the next action step, expressed as Eq. 6. Since  $\beta$  always attempt to maximize the cumulative in the future, this motivates timing taker to actively regulate the ratio of the actor-generated action to the baseline action to establish a safer action tunnel for the coming period of time, and this process must ensure the first step is safe. In the actual environment, the timing-aware action taken by the vehicle can be expressed as Eq. 7.

$$\beta(T(t)) = \frac{1 - \cos[(1 - \frac{1}{T(t)}) \cdot \pi]}{2} \quad (6)$$

$$\bar{a}(t) = \beta(T(t)) \cdot a(t) + (1 - \beta(T(t))) \cdot a_{base}(t) \quad (7)$$

Here  $T(t)$  is obtained by taking  $(s(t), a(t))$  as input, thus the timing factor  $\beta(T(t))$  computed by  $T(t)$  is generated after  $a(t)$  and denotes the timing taker's assessment of the optimal timing of executing  $a(t)$ . For training purposes, the output  $T(t)$  of timing taker is limited to a range of  $[1, T_{max}]$ . It is noteworthy that, according to Eq. 7, when  $T \rightarrow T_{max}$ , it does not necessarily mean that  $T_{max}$  is the optimal execution time of the action, but rather it indicates that the current moment should still maintain the conservative strategy to wait a better timing to act. The timing factor  $\beta(T(t))$  should be interpreted as a discounting of the future best execution time of selected action to the next step.

In the practical training of timing-aware RL, we first fix the "timing factor"  $\beta$  equal to 1 to train actor, i.e., we train a common SAC policy without considering the timing factor. When the first step of training is completed, we fix the weights of actor network and train timing taker in the "timing imagination". Then the actor and timing taker are trained in step-wise environment and "timing imagination" at the same time. The Q-function update of the actor is analogous to the general SAC policy, except that the reward obtained is for the action  $\bar{a}$  constrained by timing factor  $\beta$ . The Q function and objective function of policy network are represented by Eq. 8 and Eq. 9.

$$Q_a(s(t), a(t)) \leftarrow r(s(t), \bar{a}(t)) + \gamma \mathbb{E}_{s_{t+1} \sim P} [\hat{Q}_a(s(t+1), a(t+1))] \quad (8)$$

$$J(\phi_a) = \mathbb{E}_{s \sim D_{replay}, a \sim \pi_{\phi_a}} [Q^{\pi_{\phi_a}}(s, a) - \alpha \cdot \log \pi_{\phi_a}(a|s)] \quad (9)$$

As illustrated in Fig. 2, the agent perceives the environment with a radius of  $60m$ , and the perception range is divided into six areas: front $(-30^\circ, 30^\circ]$ , left front $(30^\circ, 90^\circ]$ , right front $(-90^\circ, -30^\circ]$ , left rear $(90^\circ, 150^\circ]$ , right rear $(-150^\circ, -90^\circ]$ , and rear $(-180^\circ, -150^\circ] \cup (150^\circ, 180^\circ]$ . In each area, the closest vehicle to the ego vehicle is selected, and the vehicle's standardized distance  $\hat{d}$ , standardized speed  $\hat{v}$ , standardized position angle  $\hat{\varphi}$ , standardized heading angle  $\hat{\theta}$  are used to described the vehicle's motion characteristics. The calculation of these variables can be seen in Eq. 10 - 13.

$$\hat{d} = \frac{d}{d_{max}} \quad (10)$$

$$\hat{v} = \frac{v}{v_{max}} \quad (11)$$

$$\hat{\varphi} = \frac{(\varphi - \varphi_{low})}{(\varphi_{high} - \varphi_{low})} \quad (12)$$

$$\hat{\theta} = \frac{\theta - \theta_{ego} + \pi}{2\pi} \quad (13)$$

Where  $d_{max}, v_{max}$  denote the maximum distance that ego vehicle can perceive and the maximum speed of the vehicle, respectively.  $\varphi_{high}, \varphi_{low}$  represent the upper and lower bounds of the position angle of each divided observation area. The calculation of relative position angle according to Eq. 12 in rear area requires a conversion into continuous angle interval, and  $\theta, \theta_{ego}$  denote the absolute heading angle of observed vehicle and ego vehicle. Then the agent's observation of its surroundings can be composed of six five-tuples.

$$s_{sur,i} = (\delta_i, \hat{d}_i, \hat{v}_i, \hat{\varphi}_i, \hat{\theta}_i), i = 1, 2, \dots, 6 \quad (14)$$

Where  $s_{sur,i}$  is the observation of the motion state of the closest surrounding vehicle in the  $i$ -th divided observation area, and  $\delta_i$  denotes whether vehicle exists in the  $i$ -th area, and takes 1 if it does, otherwise  $\delta_i = 0$ , the default value of  $s_{sur,i}$  is set to  $(0, 1, 0, 0, \frac{1}{2})$ . In addition to the observation of the surrounding vehicles, the state for RL include the state of the ego vehicle itself, which consists of two one-hot variables  $\epsilon_1, \epsilon_2$  and the standardized current ego vehicle speed  $\hat{v}_{ego}$ , expressed as Eq. 15.

$$s_{ego} = (\epsilon_1, \epsilon_2, \hat{v}_{ego}) \quad (15)$$

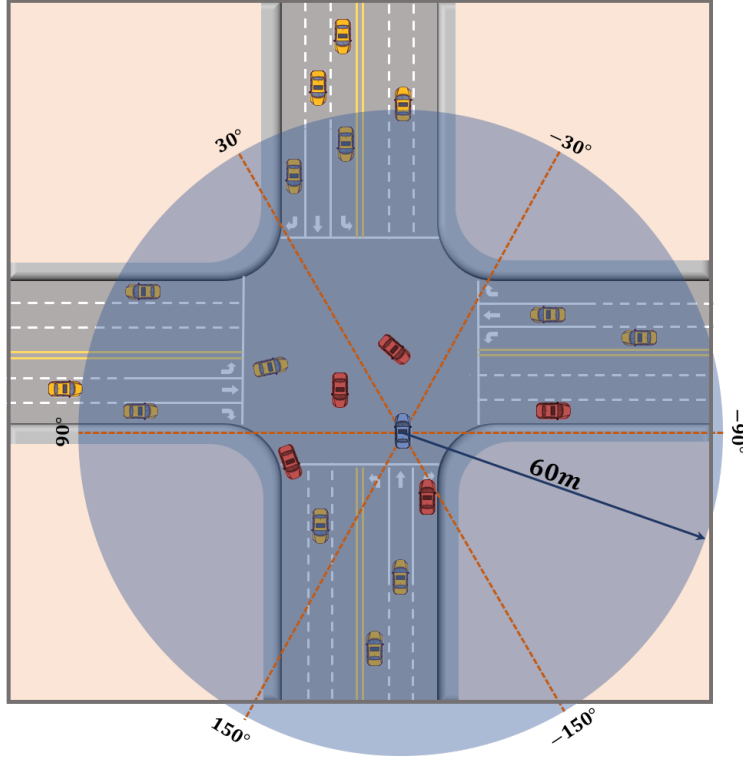


Figure 2: The observation of ego vehicle

Because in this experiment, the ego vehicle travels along the preset trajectory and only the speed needs to be planned, the heading angle of ego vehicle is not included in the  $s_{ego}$ . In Eq. 15,  $\epsilon_1$  is the one-hot vector about the ego vehicle's driving task, including going straight, turning left, and turning right,  $\epsilon_2$  is the one-hot vector about the ego vehicle's driving position, including: driving on the road before entering the intersection, being in the intersection, and exiting the intersection, and  $\hat{v}_{ego}$  can be calculated in the same way as Eq. 11. Therefore, the state of actor can be written as  $s = [s_{ego}, s_{sur,i}], i = 1, 2, \dots, 6$ , and the state of timing taker is  $[s, a]$  where  $a$  is the action produced by actor. The action ranges of actor and timing taker are  $[a_{min}, a_{max}], [1, T_{max}]$ , respectively, where  $a_{min}, a_{max}$  are the maximum deceleration and maximum acceleration of the vehicle, and the output of the timing taker is an integer value from 1 to  $T_{max}$ . In addition, the design of the reward function at each step in this study is defined as Eq. 16. When the ego car

accomplishes the driving task, it will receive a final positive reward. When the ego car collides, it will be punished. Under normal driving conditions, the ego car is incentivized to drive within a desired speed range  $[v'_{min}, v'_{max}]$ . For the timing taker, the reward of each action step is formulated as  $r'(s, a, T) = \sum_{i=0}^{T-1} \gamma^i r(s, \bar{a})$ .

$$r(s, a) = \begin{cases} 20, & \text{if ego vehicle reaches the destination} \\ -20, & \text{if ego vehicle collides} \\ \min(\frac{v_{ego} - v'_{min}}{v'_{max} - v'_{min}}, 1) \times 0.5, & \text{otherwise} \end{cases} \quad (16)$$

In the baseline model, the ego vehicle applies the Intelligent Driver Model (IDM) before driving into the intersection and after driving out of the intersection, as shown in Eq. 17-18, where  $a_{max}, v_{desire}$  denote the maximum acceleration and desired driving speed of the vehicle, respectively,  $s^*, s_0$  are the optimal following distance and the desired static distance,  $t_{desire}$  represent the desired headway, and  $b_{comf}$  is the comfortable deceleration. The above parameters of IDM are configured separately for normal road and intersection area. In the intersection scenario, the ego vehicle tends to drive in a lower desired speed and shorter following distance.  $v$  is the speed of the ego vehicle currently, and  $s, \Delta v$  denote the distance between the ego vehicle and the front vehicle and their speed difference.

$$a_{IDM} = a_{max} [1 - (\frac{v}{v_{desire}})^\delta - (\frac{s^*}{s})^2] \quad (17)$$

$$s^* = s_0 + vt_{desire} + \frac{v\Delta v}{2\sqrt{a_{max}b_{comf}}} \quad (18)$$

The baseline model sets the standard acceleration and deceleration  $a_{cross}, b_{cross}$ , as well as the set of optional crossing speed  $\mathbb{V} = \{v_1, v_2, \dots, v_n\}$  for the ego vehicle crossing the intersection, and when the ego vehicle's stop point under the standard deceleration  $b_{cross}$  is less than a certain threshold  $d_{thres}$  from the lane stop line, the ego vehicle is considered to have entered the intersection area, as expressed in Eq. 19, where  $d_{sl}$  denotes the current distance of the ego vehicle to the stop line.

$$d_{sl} - \frac{v_{ego}^2}{2 \cdot b_{cross}} \leq d_{thres} \quad (19)$$

Before approaching the lane stop line, the ego vehicle will check whether there is a potential conflict area with the surrounding vehicles, as illustrated in Fig. 3, and calculate the time for the ego vehicle to reach and leave the conflict area, expressed as Eq. 20-21, the nearest point and farthest point of conflict area to the ego vehicle are denoted as  $d_{conf, near}, d_{conf, far}$ , respectively.

$$t_{ego, arr} = f(d_{conf, near} - l_{car}/2, v_i + \Delta v, a_{req}) - \Delta t_{buffer} \quad (20)$$

$$t_{ego, leave} = f(d_{conf, far} + l_{car}/2, v_i - \Delta v, a_{req}) + \Delta t_{buffer} \quad (21)$$

Where  $f(d, s, a)$  represent the time for the vehicle to pass through a specific conflict point with distance  $d$  from current position at a constant speed  $v$  after accelerating or decelerating with acceleration  $a_{req}$ ,  $d_{conf, near} - \frac{l_{car}}{2}$ ,  $d_{conf, far} + \frac{l_{car}}{2}$  denote the distance from the front end of the vehicle to the nearest point of the conflict area, and the distance from the rear end of the vehicle to the farthest point of the conflict area, respectively, and  $v_i$  refers to the selected speed in the set of optional crossing speed  $\mathbb{V}$ . The candidate speeds in  $\mathbb{V}$  are computed in order from the highest to the lowest, and when the vehicle can cross all the conflict areas in a certain speed without conflicting with other vehicles, the corresponding speed is selected as crossing speed.  $\Delta v$  is used to take the magnitude of the possible speed fluctuation into account, and  $t_{buffer}$  is the time buffer. When current speed of the ego vehicle larger than selected speed  $v_i$ ,  $a_{req} = \min(a_{cross}, a_{IDM})$ , otherwise  $a_{req} = \min(-b_{comf}, a_{IDM})$ .

The time for the surrounding vehicles to arrive and leave the conflict area can be calculated by Eq. 22-23, where  $v_{cross, min}, v_{cross, max}, a_{cross, min}, a_{cross, max}$  denotes the optional minimum and maximum velocity, and minimum and maximum acceleration, respectively, of the surrounding vehicles as they cross the intersection. When there is an intersection of  $[t_{ego, arr}, t_{ego, leave}]$  and  $[t_{sur, arr}, t_{sur, leave}]$ , then the ego vehicle is considered to be in conflict with the surrounding vehicles, so the ego car will adopt deceleration  $b_{cross}$  to stop and wait before the stop line. Since it is possible that other vehicles stopping before the stop line may be close to the ego vehicle's travel path through the

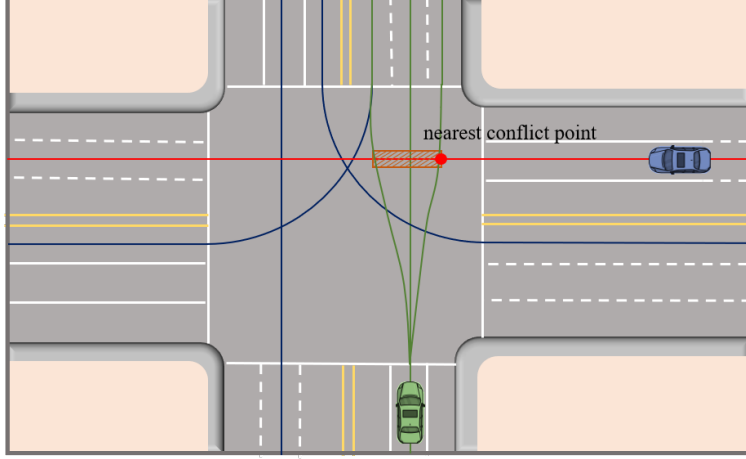


Figure 3: The conflict area between the ego vehicle and the surrounding vehicles

conflict area, causing the baseline policy to always determine that there is a conflict. Therefore, in the baseline model, the surrounding vehicles are not included in the calculation of conflict checking when they have stopped before the stop line for more than three seconds.

In addition, in the baseline model, the auto-vehicle does not always stop behind the stop line and wait; when the conflict of the surrounding vehicles decreases, it moves at a low speed to the front of the nearest of all the conflicting zones in the intersection, waits for the conflict to dissipate and then passes through the intersection, while signaling the intention to pass to the other vehicles that have not yet entered the intersection.

$$t_{sur,arr} = f(d'_{conf,near} - \frac{l_{car}}{2}, v_{cross,max}, a_{cross,max}) - \Delta t_{buffer} \quad (22)$$

$$t_{sur,leave} = f(d'_{conf,far} + \frac{l_{car}}{2}, v_{cross,min}, a_{cross,min}) + \Delta t_{buffer} \quad (23)$$

## 4 Experiment and Results

The proposed model is validated in the intersection scenario, with each direction consisting of three lanes: left turn only, straight only, and right turn only. The driving model of other vehicles in the lane is the IDM model, and the IDM parameters of each vehicle are randomly generated from a specified range, as shown in Tab. 1, to ensure sufficient behavioral diversity. The decisions of surrounding vehicles to cross the intersection or not are modeled by the Stackelberg Game [51, 52]. The first vehicle in each entrance lane participates in the game after traveling to the position where it is required to slow down in order to stop at the stop line, and the players also include the vehicles that have already stopped at the stop line. The game strategies include: "cross" or "slow down, stop and wait". If a vehicle is allowed to cross, it modifies the speed to the expected speed with given acceleration or deceleration in a personalized way. If the vehicle follows a front vehicle through the intersection, it also needs to meet the IDM model under the intersection conditions. The utility function of the game player is expressed as Eq. 24.

$$U = \sum_i \omega_i \varphi_i \quad (24)$$

Where  $\varphi_i, i = 1, 2, 3, 4$  measures the safety, efficiency, comfort and the patience of driver. The safety ( $\varphi_1$ ) is indicated by whether the current vehicle's decision to cross or stop is likely to conflict with other vehicles, if yes, then  $\varphi_1 = 1$ , otherwise  $\varphi_1 = 0$ ; The efficiency ( $\varphi_2$ ) is indicated by the expected time for the vehicle to cross the intersection; The comfort ( $\varphi_3$ ) is indicated by the deceleration required by the vehicle's decisions; The Patience ( $\varphi_4$ ) is represented by the waiting time of the vehicle at the stop line.  $w_i$  denotes the weighting coefficients of these indicators. The parameters of simulation and reinforcement learning are presented in Tab. 1.

In the experiment, we implement classic reinforcement learning as comparisons: DQN, A2C, PPO, SAC. In addition, a model-based DQN with the proposed baseline model is also included as the benchmark, where the action from



Table 1: Parameter settings

Parameters	Values	Explanations
$l_c$	5.0m	Vehicle length
$w_c$	1.8m	Vehicle width
$w_l$	3.2m	Lane width
$a_{max}$	1.5 ~ 3.0m/s <sup>2</sup>	Maximum acceleration of the vehicle
$b_{comf}$	-4.5 ~ -2.0m/s <sup>2</sup>	Comfortable deceleration of the vehicle
$\hat{v}$	8.0 ~ 12.0m/s	Target speed of car following
$\hat{d}$	6.0 ~ 12.0m	Desired car-following distance on the normal road
$\hat{d}_{cross}$	2.0 ~ 4.0m	Desired car-following distance at intersection
$a_{cross}$	2.0m/s <sup>2</sup>	Acceleration of the vehicle when crossing the intersection
$b_{cross}$	-1.5m/s <sup>2</sup>	Deceleration of the vehicle when crossing the intersection
$v_{cross}$	4.5 ~ 6.0m/s <sup>2</sup>	Target speed of the vehicle when crossing the intersection
$B$	256	Batch size of RL training
$N_{buffer}$	10 <sup>6</sup>	Size of the replay buffer in RL
$lr$	3 × 10 <sup>-4</sup>	Learning rate of RL
$N_{total}$	10 <sup>6</sup>	Total training steps of RL
$N_{start}$	2000	Sampling steps before training agents
$D_{hidden}$	[256, 256]	Dimensions of hidden layers in RL
$\gamma$	0.99	Discount factor
$\tau$	0.005	Weight coefficient for soft updating in SAC
$optimizer$	Adam	Optimizer for RL Networks

the baseline policy is added to the candidate actions of DQN, and the action with the highest value will be finally selected. The proposed model and the comparison models are trained for 10<sup>6</sup> steps, and the reward curves of the training processes are illustrated in Fig 4, the proposed model obtains the higher rewards and has a faster convergence speed compared to the other models.

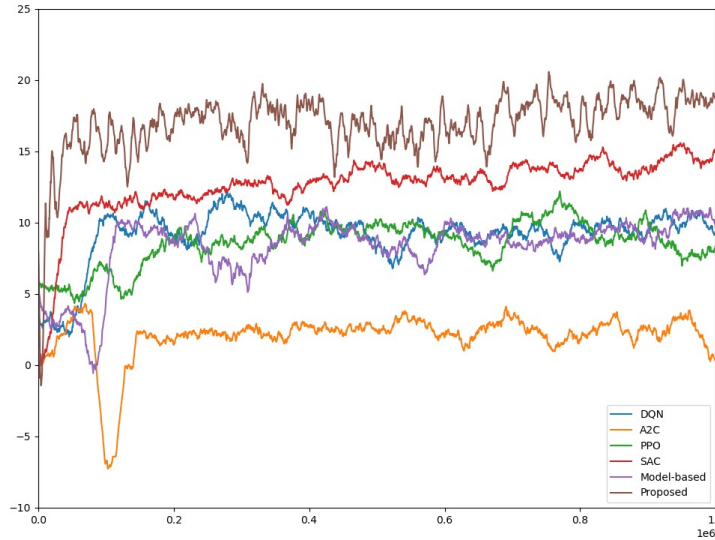


Figure 4: The reward curve of the proposed model and comparison models

After training, we compared the task success rate and the average crossing time of the proposed model and comparison models. Each model is evaluated by running 2000 episodes, and the results are presented in Tab. 2. The results demonstrate that our proposed model significantly enhances the safety and task success rate of autonomous driving in

complex interaction. The timing-aware reinforcement learning framework mitigates the "short-sighted" phenomenon of RL chasing short-term rewards when it fails to obtain the final reward during a long process, and avoids the action freezing caused by over conservative rule-based model, and ultimately significantly improves the driving safety of autonomous driving in the dense interactive scenarios.

Table 2: Experiment Results

Model Name	Success Rate	Crossing Time
DQN	64.9%	13.069 $\pm$ 5.843
A2C	64.6%	17.737 $\pm$ 10.028
PPO	65.3%	17.806 $\pm$ 9.725
SAC	67.4%	18.242 $\pm$ 10.613
Model-based DQN	73.2%	18.257 $\pm$ 10.773
Proposed	90.9%	26.155 $\pm$ 12.472

## 5 Conclusion

In this study, we propose a timing-aware reinforcement learning framework. This framework involves both an "actor" producing the best action at each step and an "timing taker" deciding the optimal execution time for the action, and the optimal execution time provides a safety constraint for every-step action through a "timing factor". The model is validated in a complex, signal-free intersection where vehicles intensively interact with each other, and compared with various mainstream and model-base reinforcement learning algorithms. The results demonstrate that the proposed method can significantly improve the safety of the task by waiting for the optimal action timing. In the future, the proposed framework can be applied to various interactive scenarios for autonomous driving, and it can also be integrated with other safe RL algorithms such as hierarchical to further improve driving safety.

## References

- [1] Shuo Feng, Haowei Sun, Xintao Yan, Haojie Zhu, Zhengxia Zou, Shengyin Shen, and Henry X Liu. Dense reinforcement learning for safety validation of autonomous vehicles. *Nature*, 615(7953):620–627, 2023.
- [2] Yihan Hu, Jiazhi Yang, Li Chen, Keyu Li, Chonghao Sima, Xizhou Zhu, Siqi Chai, Senyao Du, Tianwei Lin, Wenhai Wang, et al. Planning-oriented autonomous driving. In *Proceedings of the IEEE/CVF Conference on Computer Vision and Pattern Recognition*, pages 17853–17862, 2023.
- [3] Zhiyu Huang, Haochen Liu, Jingda Wu, and Chen Lv. Differentiable integrated motion prediction and planning with learnable cost function for autonomous driving. *IEEE transactions on neural networks and learning systems*, 2023.
- [4] David Silver, Julian Schrittwieser, Karen Simonyan, Ioannis Antonoglou, Aja Huang, Arthur Guez, Thomas Hubert, Lucas Baker, Matthew Lai, Adrian Bolton, et al. Mastering the game of go without human knowledge. *nature*, 550(7676):354–359, 2017.
- [5] Elia Kaufmann, Leonard Bauersfeld, Antonio Loquercio, Matthias Müller, Vladlen Koltun, and Davide Scaramuzza. Champion-level drone racing using deep reinforcement learning. *Nature*, 620(7976):982–987, 2023.
- [6] Zhong Cao, Kun Jiang, Weitao Zhou, Shaobing Xu, Huei Peng, and Diange Yang. Continuous improvement of self-driving cars using dynamic confidence-aware reinforcement learning. *Nature Machine Intelligence*, 5(2):145–158, 2023.
- [7] Yiren Lu, Justin Fu, George Tucker, Xinlei Pan, Eli Bronstein, Rebecca Roelofs, Benjamin Sapp, Brandyn White, Aleksandra Faust, Shimon Whiteson, et al. Imitation is not enough: Robustifying imitation with reinforcement learning for challenging driving scenarios. In *2023 IEEE/RSJ International Conference on Intelligent Robots and Systems (IROS)*, pages 7553–7560. IEEE, 2023.
- [8] Kaleb Ben Naveed, Zhiqian Qiao, and John M Dolan. Trajectory planning for autonomous vehicles using hierarchical reinforcement learning. In *2021 IEEE International Intelligent Transportation Systems Conference (ITSC)*, pages 601–606. IEEE, 2021.
- [9] Hung Duy Nguyen and Kyoungseok Han. Safe reinforcement learning-based driving policy design for autonomous vehicles on highways. *International Journal of Control, Automation and Systems*, 21(12):4098–4110, 2023.

- [10] Joshua Achiam, David Held, Aviv Tamar, and Pieter Abbeel. Constrained policy optimization. In *International conference on machine learning*, pages 22–31. PMLR, 2017.
- [11] Zhong Cao, Shaobing Xu, Huei Peng, Diange Yang, and Robert Zidek. Confidence-aware reinforcement learning for self-driving cars. *IEEE Transactions on Intelligent Transportation Systems*, 23(7):7419–7430, 2021.
- [12] Qisong Yang, Thiago D Simão, Simon H Tindemans, and Matthijs TJ Spaan. Wcsac: Worst-case soft actor critic for safety-constrained reinforcement learning. In *Proceedings of the AAAI Conference on Artificial Intelligence*, volume 35, pages 10639–10646, 2021.
- [13] Zhili Zhang, Songyang Han, Jiangwei Wang, and Fei Miao. Spatial-temporal-aware safe multi-agent reinforcement learning of connected autonomous vehicles in challenging scenarios. In *2023 IEEE International Conference on Robotics and Automation (ICRA)*, pages 5574–5580. IEEE, 2023.
- [14] David Ha and Jürgen Schmidhuber. Recurrent world models facilitate policy evolution. *Advances in neural information processing systems*, 31, 2018.
- [15] Junjie Wang, Qichao Zhang, and Dongbin Zhao. Dynamic-horizon model-based value estimation with latent imagination. *IEEE Transactions on Neural Networks and Learning Systems*, 2022.
- [16] Philipp Wu, Alejandro Escontrela, Danijar Hafner, Pieter Abbeel, and Ken Goldberg. Daydreamer: World models for physical robot learning. In *Conference on Robot Learning*, pages 2226–2240. PMLR, 2023.
- [17] Yilun Chen, Chiyu Dong, Praveen Palanisamy, Priyantha Mudalige, Katharina Mueller, and John M Dolan. Attention-based hierarchical deep reinforcement learning for lane change behaviors in autonomous driving. In *Proceedings of the IEEE/CVF Conference on Computer Vision and Pattern Recognition Workshops*, pages 0–0, 2019.
- [18] Peide Cai, Hengli Wang, Yuxiang Sun, and Ming Liu. Dq-gat: Towards safe and efficient autonomous driving with deep q-learning and graph attention networks. *IEEE Transactions on Intelligent Transportation Systems*, 23(11):21102–21112, 2022.
- [19] Meixin Zhu, Yinhai Wang, Ziyuan Pu, Jingyun Hu, Xuesong Wang, and Ruimin Ke. Safe, efficient, and comfortable velocity control based on reinforcement learning for autonomous driving. *Transportation Research Part C: Emerging Technologies*, 117:102662, 2020.
- [20] Mingfeng Yuan, Jinjun Shan, and Kevin Mi. Deep reinforcement learning based game-theoretic decision-making for autonomous vehicles. *IEEE Robotics and Automation Letters*, 7(2):818–825, 2021.
- [21] Lin Li, Wanzhong Zhao, Chunyan Wang, Abbas Fotouhi, and Xuze Liu. Nash double q-based multi-agent deep reinforcement learning for interactive merging strategy in mixed traffic. *Expert Systems with Applications*, 237:121458, 2024.
- [22] Zhiyu Huang, Jingda Wu, and Chen Lv. Efficient deep reinforcement learning with imitative expert priors for autonomous driving. *IEEE Transactions on Neural Networks and Learning Systems*, 2022.
- [23] Tejas D Kulkarni, Karthik Narasimhan, Ardavan Saeedi, and Josh Tenenbaum. Hierarchical deep reinforcement learning: Integrating temporal abstraction and intrinsic motivation. *Advances in neural information processing systems*, 29, 2016.
- [24] Hoang Le, Nan Jiang, Alekh Agarwal, Miroslav Dudík, Yisong Yue, and Hal Daumé III. Hierarchical imitation and reinforcement learning. In *International conference on machine learning*, pages 2917–2926. PMLR, 2018.
- [25] Zhangjie Cao, Erdem Bıyık, Woodrow Z Wang, Allan Raventos, Adrien Gaidon, Guy Rosman, and Dorsa Sadigh. Reinforcement learning based control of imitative policies for near-accident driving. *arXiv preprint arXiv:2007.00178*, 2020.
- [26] Junhyuk Oh, Yijie Guo, Satinder Singh, and Honglak Lee. Self-imitation learning. In *International conference on machine learning*, pages 3878–3887. PMLR, 2018.
- [27] Tong Zhou, Letian Wang, Ruobing Chen, Wenshuo Wang, and Yu Liu. Accelerating reinforcement learning for autonomous driving using task-agnostic and ego-centric motion skills. In *2023 IEEE/RSJ International Conference on Intelligent Robots and Systems (IROS)*, pages 11289–11296. IEEE, 2023.
- [28] Letian Wang, Jie Liu, Hao Shao, Wenshuo Wang, Ruobing Chen, Yu Liu, and Steven L Waslander. Efficient reinforcement learning for autonomous driving with parameterized skills and priors. *arXiv preprint arXiv:2305.04412*, 2023.
- [29] Guofa Li, Yifan Qiu, Yifan Yang, Zhenning Li, Shen Li, Wenbo Chu, Paul Green, and Shengbo Eben Li. Lane change strategies for autonomous vehicles: a deep reinforcement learning approach based on transformer. *IEEE Transactions on Intelligent Vehicles*, 2022.

- [30] Lukas M Schmidt, Sebastian Rietsch, Axel Plinge, Bjoern M Eskofier, and Christopher Mutschler. How to learn from risk: Explicit risk-utility reinforcement learning for efficient and safe driving strategies. In *2022 IEEE 25th International Conference on Intelligent Transportation Systems (ITSC)*, pages 1913–1920. IEEE, 2022.
- [31] Baiyu Peng, Jingliang Duan, Jianyu Chen, Shengbo Eben Li, Genjin Xie, Congsheng Zhang, Yang Guan, Yao Mu, and Enxin Sun. Model-based chance-constrained reinforcement learning via separated proportional-integral lagrangian. *IEEE Transactions on Neural Networks and Learning Systems*, 2022.
- [32] Ziqing Gu, Lingping Gao, Haitong Ma, Shengbo Eben Li, Sifa Zheng, Wei Jing, and Junbo Chen. Safe-state enhancement method for autonomous driving via direct hierarchical reinforcement learning. *IEEE Transactions on Intelligent Transportation Systems*, 2023.
- [33] Xuesong Wang, Jiazhi Zhang, Diyu Hou, and Yuhu Cheng. Autonomous driving based on approximate safe action. *IEEE Transactions on Intelligent Transportation Systems*, 2023.
- [34] Haitong Ma, Jianyu Chen, Shengbo Eben, Ziyu Lin, Yang Guan, Yangang Ren, and Sifa Zheng. Model-based constrained reinforcement learning using generalized control barrier function. In *2021 IEEE/RSJ International Conference on Intelligent Robots and Systems (IROS)*, pages 4552–4559. IEEE, 2021.
- [35] Richard Cheng, Gábor Orosz, Richard M Murray, and Joel W Burdick. End-to-end safe reinforcement learning through barrier functions for safety-critical continuous control tasks. In *Proceedings of the AAAI conference on artificial intelligence*, volume 33, pages 3387–3395, 2019.
- [36] Jinning Li, Liting Sun, Jianyu Chen, Masayoshi Tomizuka, and Wei Zhan. A safe hierarchical planning framework for complex driving scenarios based on reinforcement learning. In *2021 IEEE International Conference on Robotics and Automation (ICRA)*, pages 2660–2666. IEEE, 2021.
- [37] Bruno Brito, Achin Agarwal, and Javier Alonso-Mora. Learning interaction-aware guidance policies for motion planning in dense traffic scenarios. *arXiv preprint arXiv:2107.04538*, 2021.
- [38] Mohammad Al-Sharman, Rowan Dempster, Mohamed A Daoud, Mahmoud Nasr, Derek Rayside, and William Melek. Self-learned autonomous driving at unsignalized intersections: A hierarchical reinforced learning approach for feasible decision-making. *IEEE Transactions on Intelligent Transportation Systems*, 2023.
- [39] Shuojie Mo, Xiaofei Pei, and Chaoxian Wu. Safe reinforcement learning for autonomous vehicle using monte carlo tree search. *IEEE Transactions on Intelligent Transportation Systems*, 23(7):6766–6773, 2021.
- [40] Panpan Cai and David Hsu. Closing the planning–learning loop with application to autonomous driving. *IEEE Transactions on Robotics*, 39(2):998–1011, 2022.
- [41] Xiangkun He, Jingda Wu, Zhiyu Huang, Zhongxu Hu, Jun Wang, Alberto Sangiovanni-Vincentelli, and Chen Lv. Fear-neuro-inspired reinforcement learning for safe autonomous driving. *IEEE transactions on pattern analysis and machine intelligence*, 2023.
- [42] Xiangkun He and Chen Lv. Towards safe autonomous driving: Decision making with observation-robust reinforcement learning. *Automotive Innovation*, 6(4):509–520, 2023.
- [43] Weitao Zhou, Zhong Cao, Nanshan Deng, Xiaoyu Liu, Kun Jiang, and Diange Yang. Dynamically conservative self-driving planner for long-tail cases. *IEEE Transactions on Intelligent Transportation Systems*, 24(3):3476–3488, 2022.
- [44] Zhong Cao, Shaobing Xu, Xinyu Jiao, Huei Peng, and Diange Yang. Trustworthy safety improvement for autonomous driving using reinforcement learning. *Transportation research part C: emerging technologies*, 138:103656, 2022.
- [45] Yujie Yang, Yuxuan Jiang, Jianyu Chen, Shengbo Eben Li, Ziqing Gu, Yuming Yin, Qian Zhang, and Kai Yu. Belief state actor-critic algorithm from separation principle for pomdp. In *2023 American Control Conference (ACC)*, pages 2560–2567. IEEE, 2023.
- [46] Deepak Pathak, Pulkit Agrawal, Alexei A Efros, and Trevor Darrell. Curiosity-driven exploration by self-supervised prediction. In *International conference on machine learning*, pages 2778–2787. PMLR, 2017.
- [47] Yuanqing Wu, Siqin Liao, Xiang Liu, Zhihang Li, and Renquan Lu. Deep reinforcement learning on autonomous driving policy with auxiliary critic network. *IEEE transactions on neural networks and learning systems*, 34(7):3680–3690, 2021.
- [48] Jianyu Chen, Bodi Yuan, and Masayoshi Tomizuka. Model-free deep reinforcement learning for urban autonomous driving. In *2019 IEEE intelligent transportation systems conference (ITSC)*, pages 2765–2771. IEEE, 2019.
- [49] Xiaobai Ma, Jiachen Li, Mykel J Kochenderfer, David Isele, and Kikuo Fujimura. Reinforcement learning for autonomous driving with latent state inference and spatial-temporal relationships. In *2021 IEEE International Conference on Robotics and Automation (ICRA)*, pages 6064–6071. IEEE, 2021.

- [50] Jianyu Chen, Shengbo Eben Li, and Masayoshi Tomizuka. Interpretable end-to-end urban autonomous driving with latent deep reinforcement learning. *IEEE Transactions on Intelligent Transportation Systems*, 23(6):5068–5078, 2021.
- [51] Xinghao Lu, Haiyan Zhao, Cheng Li, Bingzhao Gao, and Hong Chen. A game-theoretic approach on conflict resolution of autonomous vehicles at unsignalized intersections. *IEEE Transactions on Intelligent Transportation Systems*, 2023.
- [52] Shizheng Jia, Yuxiang Zhang, Xin Li, Xiaoxiang Na, Yuhai Wang, Bingzhao Gao, Bing Zhu, and Rongjie Yu. Interactive decision-making with switchable game modes for automated vehicles at intersections. *IEEE Transactions on Intelligent Transportation Systems*, 2023.